Nanoscale

ROYAL SOCIETY OF CHEMISTRY

COMMUNICATION

View Article Online
View Journal | View Issue

Cite this: *Nanoscale*, 2020, **12**, 16046

Received 20th May 2020,
Accepted 14th July 2020

DOI: 10.1039/d0nr03891a

rsc.li/nanoscale

Size-dependent electron transfer from atomically defined nanographenes to metal oxide nanoparticles†

Peng Han, [a] Xuelin Yao,[a] Klaus Müllen, [a,b] Akimitsu Narita, [a,c] Mischa Bonn [a] and Enrique Cánovas *[a,d]

Atomically defined nanographenes (NGs) feature size-dependent energy gaps induced by, and tuneable through, quantum confinement. Their energy-tunability and robustness make NGs appealing candidates as active elements in sensitized geometries, where NGs functionalize a metal oxide (MO) film with large-area-to-volume ratio. Despite the prominent relevance of NG/MO interfaces for developing novel architectures for solar energy conversion, to date, little information is available regarding the fundamentals of electron transfer (ET) processes taking place from NG donors to MO acceptors. Here, we analyze the interplay between the size of atomically precise NGs and ET dynamics at NG/MO interfaces. We observe that as the size of NG decreases, ET from the NG donating state to the MO acceptor state speeds up. This dependence can be rationalized from variations in the donor-to-acceptor interfacial overpotential as the NG size (HOMO–LUMO gap) is reduced (increased), and can be rationalized within the framework of Marcus ET theory.

Sensitized metal oxides (MOs) represent a relevant geometry for the development of solar energy conversion schemes (*e.g.* solar cell and fuel devices). In these architectures, the sensitizers, acting as photon absorbers, enable the metal oxide to harvest photogenerated charge carriers below its generally wide insulating bandgap. The photogenerated exciton within the sensitizer can be dissociated at the sensitizer/MO interface following an electron transfer (ET) process from the sensitizer donor to the MO acceptor. Once the electron is populating the MO, it can either be extracted to an external circuit (in solar cells) or trigger chemical reactions at the MO surface (in solar fuels). From this simple description, it is clear that kinetic competition at the sensitizer/MO interfaces determines photoconversion efficiency in related devices. This aspect has been readily acknowledged for MOs sensitized by molecular dyes[1–3] and colloidal inorganic quantum dots.[4,5] The choice of a sensitizer for a given MO is critical towards photoconversion efficiency. Generally speaking, it must fulfill several requirements; the absorption onset for the sensitizer should maximize charge carrier generation upon light irradiation (*e.g.* an absorption onset of ~1.4 eV under solar irradiation[6,7]); the sensitizer/MO interfacial energetics should allow for efficient donor-to-acceptor charge transfer;[8] the sensitizer should be unaffected by photodegradation,[9] and should ideally be made of abundant and non-toxic elements.[7] To date, the most widely analyzed sensitizers for solar cell and fuel geometries are ruthenium-based organometallic dyes[10] and colloidal inorganic quantum dots (CQDs).[11,12] CQDs are characterized by larger extinction coefficients when compared with Ru-based dyes, enabling thinner devices and hence reducing device costs. Importantly, and unique to CQDs, their optoelectronic properties, such as absorption onset and workfunction, can be finely tuned by controlling their size and surface composition.[13] A drawback of CQDs, when compared with molecular dyes, is the requirement for efficient surface passivation schemes,[13] complicating sensitizer/MO interfacial chemistry and introducing non-radiative recombination pathways within the sensitizer, which can have a detrimental impact in photoconversion efficiency. A troublesome issue regarding both sensitizers (Ru-based dyes and CQDs) refers to the common employment of toxic and expensive elements on their synthesis. Recently, nanographenes (NGs), large polycyclic aromatic hydrocarbons (*i.e.*, with size >1 nm), also referred to as graphene quantum dots, have been introduced as an appealing alternative to conventional sensitizers.[14–16] NGs, while being metal-free molecular sensitizers, display larger extinc-

[a]*Max Planck Institute for Polymer Research, Ackermannweg 10, 55128 Mainz, Germany. E-mail: enrique.canovas@imdea.org*
[b]*Institute of Physical Chemistry, Johannes Gutenberg University Mainz, Duesbergweg 10-14, 55128 Mainz, Germany*
[c]*Organic and Carbon Nanomaterials Unit, Okinawa Institute of Science and Technology Graduate University, Okinawa 904-0495, Japan*
[d]*Instituto Madrileño de Estudios Avanzados en Nanociencia (IMDEA Nanociencia), Faraday 9, 28049 Madrid, Spain*

†Electronic supplementary information (ESI) available: Sample preparation; Definition of size: percentage of compactness; Absorption and emission spectra; Estimation of ET driving force for thermalized and nonthermalized electrons; Absorption for sensitized electrodes. See DOI: 10.1039/d0nr03891a

tion coefficients and higher stability when compared with conventional dyes.[17] Notably NGs, defined by atomically precise structures, feature finite size-dependent energy gaps induced by quantum confinement effects.[18–20] While this feature parallels the observables made for inorganic CQDs, the achievable monodisperse molecular character for atomically precise NGs make their gaps to be uniquely defined (unlike their inorganic counterparts where a distribution of sizes is often obtained). Furthermore, apart from the exquisite control that can be achieved over their sizes, edge structures of NGs can be also tailored and even functionalized;[18,19] factors that further allow for fine-tuning of their optoelectronic properties.[21–24] These combined features make NGs very appealing candidates as sensitizers of MO electrodes.

Despite the relevance of NG/MO interfaces for developing novel solar energy conversion architectures, to date, little information is available regarding the fundamentals of ET process from NG donors to MO acceptors (that, as stated previously, do determine the photoconversion efficiency in related devices). In this work, we analyze the interplay between the size of atomically precise NGs and related ET dynamics at NG/MO interfaces. We resolve that as the size of NG decreases, the ET rates between the NG donor and MO acceptor become faster, a result that is rationalized within Marcus theory. These results demonstrate that the selection of a given size and edge of NG sensitizer (with a defined absorption onset) determines ET process efficiency, the latter being determined by the kinetic competition between ET towards the oxide electrode and competing decay channels at the NG/MO interface.

The set of molecular NGs structures used in this study are summarized in Fig. 1a. These NGs were synthesized through oxidative cyclodehydrogenation of corresponding tailor-made polyphenylene precursors, following our previously reported procedures.[19,25–29] In this work, we name our samples as *C#*/*R*, where *C#* denotes the number of carbons contained in the core structure and *R* the number of fused rings. Note that many NG configurations are possible for a given number of carbons and/or rings, these has been previously categorized by the percentage of compactness (degree of condensation) ranging between 0% (cata-compounds) up to 100% for pure *peri*-condensed systems.[18] The set of samples analyzed here are characterized by a high degree of compactness, with figures ranging between 81 and 87% (see ESI†). Fig. 1b shows as square open dots, the dependence of highest occupied molecular orbital (HOMO)-lowest unoccupied molecular orbital (LUMO) gaps (ΔE_{H-L}) as a function of NG number of fused rings, inferred from absorption measurements for the analyzed set of samples dispersed in toluene (see ESI†). Fig. 1b also presents, as blue open stars, the theoretical estimates calculated from ZINDO/S on NGs for pure *peri*-condensed (circular) systems.[18] The results are consistent with the dependence expected for a quantum-mechanical particle in a two-dimensional box, where the energies scale with the area of the box; in this case the number of fused rings *R*. A global fit to all the data (including open stars and squares) provides an overall relationship between NG HOMO–LUMO gap and number of fused carbon rings of $\Delta E_{H-L} = 5.46(\pm 0.2)R^{-0.30\pm0.01}$, in good agreement with theoretical estimates.[18,30–32]

Mesoporous metal oxide films (~10 μm thick) from SnO_2 nanopowders (≤100 nm average particle size, Sigma-Aldrich ref# 549657) were deposited onto 1 mm thick fused silica substrates by the doctor blading technique and sintered at 450 C for 2 h. The resulting MO films were sensitized with NGs defined by different sizes by immersing them for 12 h in dispersions of NGs in toluene. The films were subsequently rinsed several times with toluene to remove any excess of NGs not adsorbed to the MO surface (the absorbance of sensitized samples is given in the ESI†). Interfacial ET rates in these sensitized films were subsequently determined using optical pump-THz probe (OPTP) spectroscopy; sample preparation

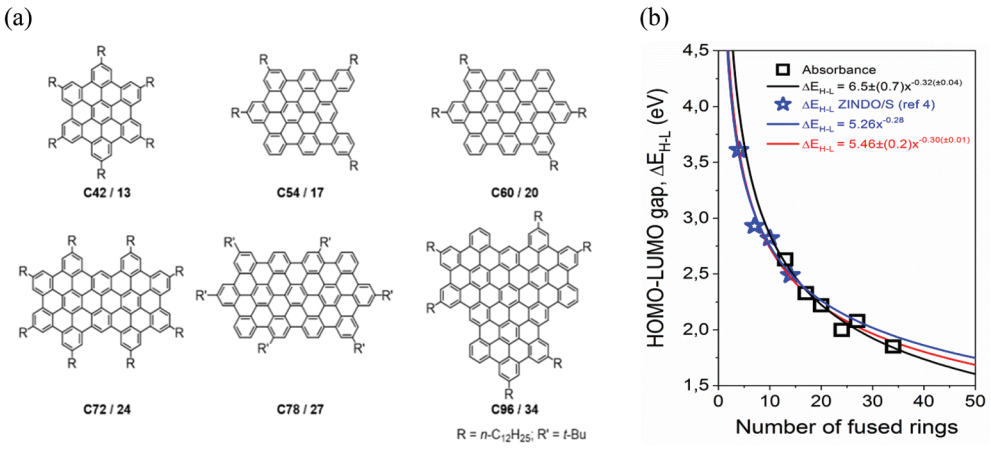

Fig. 1 (a) Chemical structures of the NGs analyzed in this work. The samples are labelled as *C#*/*R*, where # denotes the number of carbons contained in the core structure and *R* the number of fused rings. (b) HOMO–LUMO gap inferred from absorption spectra, as black open squares, as a function of number of fused carbon rings for the samples sketched in panel a (dispersed in toluene). The theoretical estimates calculated from ZINDO/S on NGs with 100% compactness[18] are shown as blue open stars. The red line represents a power law dependent global fit (see main text) to the presented data.

and measurements were performed under nitrogen atmosphere.

We and others have previously demonstrated the unique suitability of OPTP spectroscopy to quantify ultrafast interfacial ET dynamics in dye[9,33–36] and QD[37–39] sensitized oxide systems. OPTP is capable of time-resolving the evolution of the photoconductivity of a given system following above-bandgap optical excitation with sub-ps resolution and in a contactless fashion.[40] The ~2 THz bandwidth probe pulse is primarily sensitive to free carrier motion (*i.e.* photoconductivity, $\sigma = q \times N \times \mu$, where q is the electron charge, N the number of absorbed photons and μ the mobility of photogenerated carriers). The OPTP signal is insensitive to excitons in NGs and therefore neatly probes the emergence of photoconductivity in the MO electrode after selective optical excitation of the sensitizer. As such, OPTP traces reveal the arrival of electrons from the sensitizer's populated molecular orbitals (*e.g.* LUMO) into the oxide's conduction band (CB); that is, it resolves unambiguously the ET process from the NG donor to the MO acceptor.

Fig. 2a shows normalized OPTP dynamics for the samples analyzed in this study. The samples were excited at 400 nm with a fluence of 40 μJ cm^{-2}. This fluence ensured single excitation in NGs; the wavelength guaranteed selective excitation of NGs. No OPTP response was observed for a bare mesoporous SnO_2 film, demonstrating that the signal presented in Fig. 2a only reflects ET from the NG donor to the MO acceptor. As evident from Fig. 2a, the sensitization of mesoporous SnO_2 by the NGs sensitizers – physisorbed at the oxide surface[41] – provides biphasic dynamics in all the cases. As such, all the OPTP line traces can be well described by a bi-exponential ET model (solid lines in Fig. 2a). A summary of the deduced ET rate constants as a function of NG number of fused carbon rings is shown in Fig. 2b, where black open circles and blue open diamonds represent the fast and slow ET rate constants for each sensitizer. From the plot it is clear that ET dynamics are slowed down as the NG size increases; this applies to both rate constants (the fast and slow components). Qualitatively, this result can be rationalized by taking into account that reduced NG sizes are characterized by larger optical energy gaps (see Fig. 1). This feature promotes larger excess energy offsets between donating and accepting states at the NG/MO interface (*i.e.* larger driving energy for ET, generally denoted as ΔG). Such dependence, which has been previously reported in other MO systems sensitized with dyes[42–44] and inorganic colloidal quantum dots,[39,45] can be modeled using Marcus theory (see below). On the other hand, biphasic ET dynamics have been previously reported for dye- and QD-sensitized oxide systems,[43,46–51] and in a recent paper by us analyzing the role of physisorption and chemisorption at NGs/MO interfaces.[41] Bi-phasic dynamics indicate two distinct transfer channels from the NGs towards the oxide electrode. In the following, we discuss the probable origin for the biphasic nature of the process.

Our previous work analyzing ET rates on colloidal inorganic quantum dots (CQDs) sensitizing the same MO electrode (Sigma-Aldrich, ref# 549657) revealed that ET from the CQD LUMO to the MO was always well characterized by a monophasic ET component for systems where intra-band CQD relaxation within the sensitizer was kinetically faster than ET towards the oxide.[39,52] When CQD hot-electron intraband relaxation was kinetically competing with ET, bi-phasic ET dynamics were obtained from, respectively, hot and cold electrons populating the sensitizer.[37,53] The relative weight of hot and cold ET was determined by CQD intra-band relaxation kinetics. Beyond inorganic CQDs, hot and cold ET has also been reported in dye/MO systems,[44,54] and has been related by several authors, in first approximation, with the presence of a frequency offset between dye absorption and emission.[55,56] An energy onset between absorption and emission might indicate that, after photon absorption in the NG, there is substantial energy relaxation within the sensitizer prior to radiative emission. Under these circumstances, the relative rate of this intramolecular relaxation process *vs.* ET towards the oxide will determine whether hot ET towards the MO is possible in a given system. All NGs in this work exhibit a large Stokes shift (see ESI†), this alone might support the scenario where ET toward the MO is taking place from hot and cold states in the analyzed NGs. Furthermore, this hypothesis is consistent with

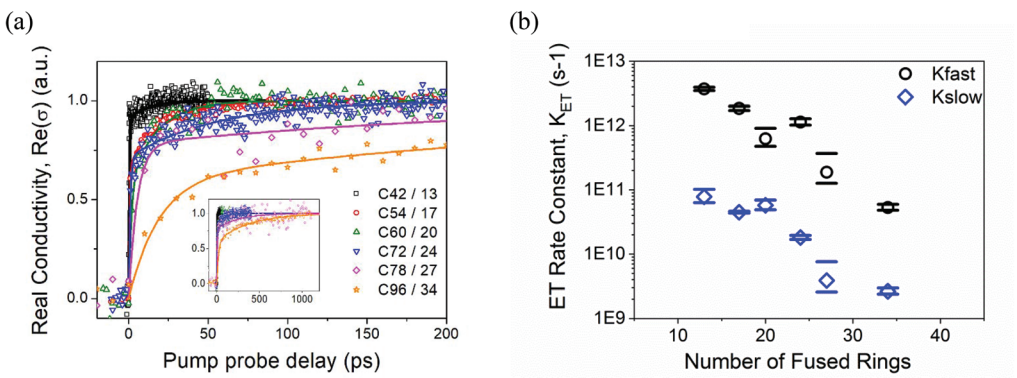

Fig. 2 (a) Normalized OPTP dynamics from different sized NGs to the MO electrode. Solid lines are bi-exponential fits. The inset shows the same kinetics over a 1 ns time window. (b) ET rate constants *vs.* the number of NG fused rings for the fast (black dots) and slow (blue dots) kinetic components.

previous reports analyzing carrier dynamics on NGs, where carrier cooling has been reported to be rather slow (with hot-electron lifetimes as long as ~100 ps for C132/48 NGs[57]). Hot electrons in NGs do have a large probability of emitting both phosphorescence and fluorescence at room temperature.[57–59] Indeed, the long lifetimes of hot carriers in NGs have allowed researchers to demonstrate efficient sub-ps hot-electron transfer in C132 NG sensitizing a planar TiO_2(110) rutile surface.[60] Taking into account the discussion made above, we rationalize the presence of slow and fast components in NG/MO interfacial OPTP dynamics with cold and hot ET transfer components inherently linked to each NG sensitizer. That is, in first approximation cold ET is assumed to take place from the absorption ground state (following intramolecular vibrational relaxation) while hot ET takes place prior to any energy dissipation process taking place within the NG.

Assuming that the biphasic nature of the process is linked with hot and cold ET channels, we model our results within the Marcus theory. Following this model, the rate constant (k_{ET}) of electron transfer between a localized donor state towards an accepting continuum of states can be expressed as:[43]

$$k_{ET} = \frac{2\pi}{\hbar}\int_0^{\Delta G} dE\rho(E)|H_{DA}(E)|^2 \frac{1}{\sqrt{4\pi\lambda k_B T}} e^{-\frac{(\lambda-\Delta G+E)^2}{4\lambda k_B T}} \quad (1)$$

where the ET rate for a given temperature (T) is defined by: (1) ΔG, the energy difference between donating state and the bottom of the accepting MO conduction band, commonly referred as the ET driving force; (2) $|H_{DA}(E)|^2$, the coupling strength, which reflects the wavefunction overlap between donor and acceptor states; (3) $\rho(E)$, the density of states in the conduction band of the acceptor; and (4) λ, the reorganizational energy that accounts for energy fluctuations in the systems due to charge transfer. To model the kinetic data presented in Fig. 2b by eqn (1), we approximate the density of MO accepting states by an $E^{1/2}$ dependence. The wave function overlap $|H_{AB}(E)|^2$ between donating and accepting states is assumed to follow a power-law relationship with energy.[39] As the bi-phasic ET dynamics are interpreted here as hot and cold ET channels, we need to define ΔG_{cold} and ΔG_{hot} for each sensitizer. For the slow component, we infer ΔG_{cold} conventionally as the energy onset between NG LUMO (obtained from gas phase DFT, see ESI†) and the SnO_2 CB workfunctions (estimated from ultraviolet photoelectron spectroscopy[41]). For the fast component, ΔG_{hot} is deduced as $\Delta G_{hot} = \Delta G_{cold} + (h\nu^{pump} - \Delta E_{H-L})$ (where $h\nu^{pump}$ refers to the employed 400 nm photon pump energy). Fig. 3 summarizes the resolved ET rate constants (for hot and cold components) as a function of derived ΔGs. The red line in Fig. 3 represents the best description of the data using eqn (1). Apart from a scaling factor, the only adjustable parameter in eqn (1) is the reorganizational energy, which is found to be $\lambda = 1 \pm 50$ meV for the analyzed system. This small value is in very good agreement with the results obtained for inorganic CQDs sensitizing MOs,[39,48] and will imply that vibronic and solvation effects do not significantly affect ET in the studied systems. The theoretical curve describes the experimental data fairly well, suggesting the validity of the Marcus model for describing ET at NG/MO interfaces. In any case, it is clear from Fig. 3 that further work is needed to fully validate whether Marcus model applies or not for these systems. Particularly, studying ET for even larger molecules (smaller gaps) might provide a larger range of ΔG values and therefore a more reliable fit to the model. Furthermore, a better description for the interaction between NG and oxide is also needed in order to accurately determine ΔGs. Finally, an analysis for the temperature dependence of ET *vs.* NG size might offer insights on the adiabatic or non-adiabatic nature of the process. All these studies are underway in our labs and will be reported elsewhere.

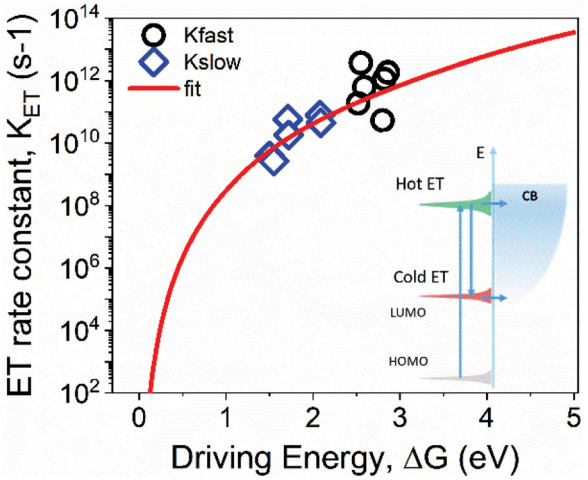

Fig. 3 ET rate constants as a function of the ET driving energy ΔG for the fast and slow components (black and blue dots respectively). In the inset we show an scheme illustrating these two channels at the interface between NG and MO.

In summary, size-dependent ET rates from nanographenes to metal oxide nanoparticles reveals two ET channels, which can be rationalized by hot and cold ET processes. The dependence of ET rates on NG size can be reasonably well described by Marcus theory, where ET rates from the NG towards the MO become faster as the NG size is reduced (*i.e.* as the energy gap of the NGs become larger). Regarding the exploitation of NG/MO interfaces in photocatalytic and photovoltaic devices, it is worth commenting that faster ET processes enabled by smaller NGs (larger bandgaps and then ΔG over-potentials) will not necessarily be the best recipe. First, to boost charge carrier collection under solar illumination, one should select larger NGs, which possess smaller gaps, with an optimum of 1.4 eV following the Shockley–Queisser limit (that is for NGs made *peri*-condensed systems made of ~50 fused rings, see Fig. 1b). However, as evident from our results, larger NGs exhibit lower ET rates (K_{ET}) that might eventually compete with *e.g.* radiative relaxation (K_{rad}) within the NGs, thereby reducing the electron collection efficiency. Clearly, a compromise between absorption onset and NG/MO interfacial ET must be found; the optimum will be defined by the NG revealing the narrowest HOMO–LUMO gap while keeping $K_{ET} \gg K_{rad}$.

Author contributions

P.H. and E.C. conceived and designed the study. X.L.Y. prepared and characterized the nanographenes. X.L.Y. and A.N. performed the gas-phase DFT calculations. P.H. sensitized the nanographenes onto metal oxides and conducted OPTP experiments. P.H. and E.C. analyzed the data. All authors contributed to writing the paper.

Conflicts of interest

The authors declare no competing financial interests.

Acknowledgements

This work was funded by the Max Planck Society. Enrique Cánovas acknowledges financial support from the regional government of Comunidad de Madrid under projects 2017-T1/AMB-5207 & P2018/NMT-4511, and the "Severo Ochoa" Programme for Centres of Excellence in R&D (MINECO, Grant No. SEV-2016-0686). Open Access funding provided by the Max Planck Society

References

1 R. E. Bangle and G. J. Meyer, Factors That Control the Direction of Excited-State Electron Transfer at Dye-Sensitized Oxide Interfaces, *J. Phys. Chem. C*, 2019, **123**(42), 25967–25976.
2 M. Soroush and K. K. S. Lau, *Dye-Sensitized Solar Cells: Mathematical Modelling, and Materials Design and Optimization*, 2019.
3 M. K. Nazeeruddin, E. Baranoff and M. Grätzel, Dye-Sensitized Solar Cells: A Brief Overview, *Sol. Energy*, 2011, **85**(6), 1172–1178.
4 E. H. Sargent, Colloidal Quantum Dot Solar Cells, *Nat. Photonics*, 2012, **6**(3), 133–135.
5 H. Dong, F. Xu, Z. Sun, X. Wu, Q. Zhang, Y. Zhai, X. D. Tan, L. He, T. Xu, Z. Zhang, *et al.*, In Situ Interface Engineering for Probing the Limit of Quantum Dot Photovoltaic Devices, *Nat. Nanotechnol.*, 2019, **14**(10), 950–956.
6 M. G. Walter, E. L. Warren, J. R. McKone, S. W. Boettcher, Q. Mi, E. A. Santori and N. S. Lewis, Solar Water Splitting Cells, *Chem. Rev.*, 2010, **110**(11), 6446–6473.
7 A. Hagfeldt, G. Boschloo, L. Sun, L. Kloo and H. Pettersson, Dye-Sensitized Solar Cells, *Chem. Rev.*, 2010, **110**(11), 6595–6663.
8 A. Listorti, B. O'Regan and J. R. Durrant, Electron Transfer Dynamics in Dye-Sensitized Solar Cells, *Chem. Mater.*, 2011, **23**(15), 3381–3399.
9 M. Karakus, W. Zhang, H. J. Räder, M. Bonn and E. Cánovas, Electron Transfer from Bi-Isonicotinic Acid Emerges upon Photodegradation of N3-Sensitized TiO_2 Electrodes, *ACS Appl. Mater. Interfaces*, 2017, **9**(40), 35376–35382.
10 Y. Qin and Q. Peng, Ruthenium Sensitizers and Their Applications in Dye-Sensitized Solar Cells, *Int. J. Photoenergy*, 2012, **2012**, 1–21.
11 I. J. Kramer and E. H. Sargent, Colloidal Quantum Dot Photovoltaics: A Path Forward, *ACS Nano*, 2011, **5**(11), 8506–8514.
12 G. Konstantatos and E. H. Sargent, in *Colloidal Quantum Dot Optoelectronics and Photovoltaics*, ed. G. Konstantatos and E. H. Sargent, Cambridge University Press, Cambridge, 2013, vol. 9780521198.
13 H. Zhong, Z. Bai and B. Zou, Tuning the Luminescence Properties of Colloidal I–III–VI Semiconductor Nanocrystals for Optoelectronics and Biotechnology Applications, *J. Phys. Chem. Lett.*, 2012, **3**(21), 3167–3175.
14 T. Majumder, S. Dhar, K. Debnath and S. P. Mondal, Role of S, N Co-Doped Graphene Quantum Dots as a Green Photosensitizer with Ag-Doped ZnO Nanorods for Improved Electrochemical Solar Energy Conversion, *Mater. Res. Bull.*, 2017, **93**, 214–222.
15 S. Kundu, P. Sarojinijeeva, R. Karthick, G. Anantharaj, G. Saritha, R. Bera, S. Anandan, A. Patra, P. Ragupathy, M. Selvaraj, *et al.* Enhancing the Efficiency of DSSCs by the Modification of TiO_2 Photoanodes Using N, F and S, Co-Doped Graphene Quantum Dots, *Electrochim. Acta*, 2017, **242**, 337–343.
16 Y. Zhang, F. Qi, Y. Li, X. Zhou, H. Sun, W. Zhang, D. Liu and X.-M. Song, Graphene Oxide Quantum Dot-Sensitized Porous Titanium Dioxide Microsphere: Visible-Light-Driven Photocatalyst Based on Energy Band Engineering, *J. Colloid Interface Sci.*, 2017, **498**, 105–111.
17 X. Yan, X. Cui, B. Li and L.-S. Li, Large, Solution-Processable Graphene Quantum Dots as Light Absorbers for Photovoltaics, *Nano Lett.*, 2010, **10**(5), 1869–1873.
18 Y. Ruiz-Morales, HOMO-LUMO Gap as an Index of Molecular Size and Structure for Polycyclic Aromatic Hydrocarbons (PAHs) and Asphaltenes: A Theoretical Study. I, *J. Phys. Chem. A*, 2002, **106**(46), 11283–11308.
19 F. Dötz, J. D. Brand, S. Ito, L. Gherghel and K. Müllen, Synthesis of Large Polycyclic Aromatic Hydrocarbons: Variation of Size and Periphery, *J. Am. Chem. Soc.*, 2000, **122**(32), 7707–7717.
20 G. Malloci, G. Cappellini, G. Mulas and A. Mattoni, Electronic and Optical Properties of Families of Polycyclic Aromatic Hydrocarbons: A Systematic (Time-Dependent) Density Functional Theory Study, *Chem. Phys.*, 2011, **384**(1–3), 19–27.
21 S. H. Song, M.-H. Jang, J. Chung, S. H. Jin, B. H. Kim, S.-H. Hur, S. Yoo, Y.-H. Cho and S. Jeon, Highly Efficient Light-Emitting Diode of Graphene Quantum Dots Fabricated from Graphite Intercalation Compounds, *Adv. Opt. Mater.*, 2014, **2**(11), 1016–1023.
22 Z. Wang, F. Yuan, X. Li, Y. Li, H. Zhong, L. Fan and S. Yang, 53% Efficient Red Emissive Carbon Quantum Dots

for High Color Rendering and Stable Warm White-Light-Emitting Diodes, *Adv. Mater.*, 2017, **29**(37), 1702910.

23 M. Dutta, S. Sarkar, T. Ghosh and D. Basak, ZnO/Graphene Quantum Dot Solid-State Solar Cell, *J. Phys. Chem. C*, 2012, **116**(38), 20127–20131.

24 B. Y. Zhang, T. Liu, B. Meng, X. Li, G. Liang, X. Hu and Q. J. Wang, Broadband High Photoresponse from Pure Monolayer Graphene Photodetector, *Nat. Commun.*, 2013, **4**(1), 1–11.

25 Ž Tomović, M. D. Watson and K. Müllen, Superphenalene-Based Columnar Liquid Crystals, *Angew. Chem., Int. Ed.*, 2004, **43**(6), 755–758.

26 T. Böhme, C. D. Simpson, K. Müllen and J. P. Rabe, Current–Voltage Characteristics of a Homologous Series of Polycyclic Aromatic Hydrocarbons, *Chem. – Eur. J.*, 2007, **13**(26), 7349–7357.

27 D. Wasserfallen, M. Kastler, W. Pisula, W. A. Hofer, Y. Fogel, Z. Wang and K. Müllen, Suppressing Aggregation in a Large Polycyclic Aromatic Hydrocarbon, *J. Am. Chem. Soc.*, 2006, **128**(4), 1334–1339.

28 V. S. Iyer, K. Yoshimura, V. Enkelmann, R. Epsch, J. P. Rabe and K. Müllen, A Soluble C60 Graphite Segment, *Angew. Chem., Int. Ed.*, 1998, **37**(19), 2696–2699.

29 A. Stabel, P. Herwig, K. Müllen and J. P. Rabe, Diodelike Current–Voltage Curves for a Single Molecule–Tunneling Spectroscopy with Submolecular Resolution of an Alkylated,Peri-Condensed Hexabenzocoronene, *Angew. Chem., Int. Ed. Engl.*, 1995, **34**(15), 1609–1611.

30 H. Li, X. He, Z. Kang, H. Huang, Y. Liu, J. Liu, S. Lian, C. H. A. Tsang, X. Yang and S. T. Lee, Water-Soluble Fluorescent Carbon Quantum Dots and Photocatalyst Design, *Angew. Chem., Int. Ed.*, 2010, **49**(26), 4430–4434.

31 A. D. Güçlü, P. Potasz and P. Hawrylak, Excitonic Absorption in Gate-Controlled Graphene Quantum Dots, *Phys. Rev. B: Condens. Matter Mater. Phys.*, 2010, **82**(15), 155445.

32 G. Eda, Y. Y. Lin, C. Mattevi, H. Yamaguchi, H. A. Chen, I. S. Chen, C. W. Chen and M. Chhowalla, Blue Photoluminescence from Chemically Derived Graphene Oxide, *Adv. Mater.*, 2010, **22**(4), 505–509.

33 G. M. Turner, M. C. Beard and C. A. Schmuttenmaer, Carrier Localization and Cooling in Dye-Sensitized Nanocrystalline Titanium Dioxide, *J. Phys. Chem. B*, 2002, **106**(45), 11716–11719.

34 P. Tiwana, P. Docampo, M. B. Johnston, H. J. Snaith and L. M. Herz, Electron Mobility and Injection Dynamics in Mesoporous ZnO, SnO_2, and TiO_2 Films Used in Dye-Sensitized Solar Cells, *ACS Nano*, 2011, **5**(6), 5158–5166.

35 P. Tiwana, P. Parkinson, M. B. Johnston, H. J. Snaith and L. M. Herz, Ultrafast Terahertz Conductivity Dynamics in Mesoporous TiO_2 : Influence of Dye Sensitization and Surface Treatment in Solid-State Dye-Sensitized Solar Cells, *J. Phys. Chem. C*, 2010, **114**(2), 1365–1371.

36 J. C. Brauer and J.-E. Moser, Transient Photoconductivity of Dye-Sensitized TiO_2 Nanocrystalline Films Probed by Optical Pump-THz Probe Spectroscopy, *Ultrafast Phenom. XVII*, 2011, 358–360.

37 H. Wang, I. Barceló, T. Lana-Villarreal, R. Gómez, M. Bonn and E. Cánovas, Interplay Between Structure, Stoichiometry, and Electron Transfer Dynamics in SILAR-Based Quantum Dot-Sensitized Oxides, *Nano Lett.*, 2014, **14**(10), 5780–5786.

38 K. Zhao, Z. Pan, I. Mora-Sero, E. Canovas, H. Wang, Y. Song, X. Gong, J. Wang, M. Bonn, J. Bisquert, *et al.* Boosting Power Conversion Efficiencies of Quantum-Dot-Sensitized Solar Cells Beyond 8% by Recombination Control, *J. Am. Chem. Soc.*, 2015, **137**(16), 5602–5609.

39 E. Cánovas, P. Moll, S. A. Jensen, Y. Gao, A. J. Houtepen, L. D. A. Siebbeles, S. Kinge and M. Bonn, Size-Dependent Electron Transfer from PbSe Quantum Dots to SnO_2 Monitored by Picosecond Terahertz Spectroscopy, *Nano Lett.*, 2011, **11**(12), 5234–5239.

40 R. Ulbricht, E. Hendry, J. Shan, T. F. Heinz and M. Bonn, Carrier Dynamics in Semiconductors Studied with Time-Resolved Terahertz Spectroscopy, *Rev. Mod. Phys.*, 2011, **83**(2), 543–586.

41 P. Han, I. C.-Y. Hou, H. Lu, X.-Y. Wang, K. Müllen, M. Bonn, A. Narita and E. Cánovas, Chemisorption of Atomically Precise 42-Carbon Graphene Quantum Dots on Metal Oxide Films Greatly Accelerates Interfacial Electron Transfer, *J. Phys. Chem. Lett.*, 2019, 1431–1436.

42 N. A. Anderson and T. Lian, Ultrafast Electron Transfer At the Molecule-Semiconductor Nanoparticle Interface, *Annu. Rev. Phys. Chem.*, 2005, **56**(1), 491–519.

43 J. B. Asbury, E. Hao, Y. Wang, H. N. Ghosh and T. Lian, Ultrafast Electron Transfer Dynamics from Molecular Adsorbates to Semiconductor Nanocrystalline Thin Films, *J. Phys. Chem. B*, 2001, **105**(20), 4545–4557.

44 M. Ziółek, B. Cohen, X. Yang, L. Sun, M. Paulose, O. K. Varghese, C. A. Grimes and A. Douhal, Femtosecond to Millisecond Studies of Electron Transfer Processes in a Donor-(π-Spacer)-Acceptor Series of Organic Dyes for Solar Cells Interacting with Titania Nanoparticles and Ordered Nanotube Array Films, *Phys. Chem. Chem. Phys.*, 2012, **14**(8), 2816–2831.

45 I. Robel, M. Kuno and P. V. Kamat, Size-Dependent Electron Injection from Excited CdSe Quantum Dots into TiO_2 Nanoparticles, *J. Am. Chem. Soc.*, 2007, **129**(14), 4136–4137.

46 K. Žídek, K. Zheng, C. S. Ponseca, M. E. Messing, L. R. Wallenberg, P. Chábera, M. Abdellah, V. Sundström and T. Pullerits, Electron Transfer in Quantum-Dot-Sensitized ZnO Nanowires: Ultrafast Time-Resolved Absorption and Terahertz Study, *J. Am. Chem. Soc.*, 2012, **134**(29), 12110–12117.

47 Y. Yang, W. Rodríguez-Córdoba, X. Xiang, T. Lian, W. Rodriguez-Cordoba, X. Xiang and T. Lian, Strong Electronic Coupling and Ultrafast Electron Transfer between PbS Quantum Dots and TiO_2 Nanocrystalline Films, *Nano Lett.*, 2012, **12**(1), 303–309.

48 K. Tvrdy, P. A. Frantsuzov and P. V. Kamat, Photoinduced Electron Transfer from Semiconductor Quantum Dots to Metal Oxide Nanoparticles, *Proc. Natl. Acad. Sci. U. S. A.*, 2011, **108**(1), 29–34.

49 R. L. Milot, G. F. Moore, R. H. Crabtree, G. W. Brudvig and C. A. Schmuttenmaer, Electron Injection Dynamics from Photoexcited Porphyrin Dyes into SnO_2 and TiO_2 Nanoparticles, *J. Phys. Chem. C*, 2013, **117**(42), 21662–21670.

50 R. S. Dibbell, D. G. Youker and D. F. Watson, Excited-State Electron Transfer from CdS Quantum Dots to TiO_2 Nanoparticles via Molecular Linkers with Phenylene Bridges, *J. Phys. Chem. C*, 2009, **113**(43), 18643–18651.

51 J. L. Blackburn, D. C. Selmarten and A. J. Nozik, Electron Transfer Dynamics in Quantum Dot/Titanium Dioxide Composites Formed by in Situ Chemical Bath Deposition, *J. Phys. Chem. B*, 2003, **107**(51), 14154–14157.

52 H. Wang, E. R. McNellis, S. Kinge, M. Bonn and E. Cánovas, Tuning Electron Transfer Rates through Molecular Bridges in Quantum Dot Sensitized Oxides, *Nano Lett.*, 2013, **13**(11), 5311–5315.

53 H. I. Wang, I. Infante, S. T. Brinck, E. Cánovas and M. Bonn, Efficient Hot Electron Transfer in Quantum Dot-Sensitized Mesoporous Oxides at Room Temperature, *Nano Lett.*, 2018, **18**(8), 5111–5115.

54 S. Ardo and G. J. Meyer, Photodriven Heterogeneous Charge Transfer with Transition-Metal Compounds Anchored to TiO_2 Semiconductor Surfaces, *Chem. Soc. Rev.*, 2009, **38**(1), 115–164.

55 S. Iwai, K. Hara, R. Katoh, S. Murata, H. Sugihara and H. Arakawa, Ultrafast Interfacial Charge Separation from the Singlet and Triplet MLCT States of $Ru(Bpy)_2(Dcbpy)$ Adsorbed on Nanocrystalline SnO_2 under Applied Bias, in *Springer Series in Chemical Physics*, 2001, vol. 66, pp. 447–449.

56 O. Bräm, A. Cannizzo and M. Chergui, Ultrafast Fluorescence Studies of Dye Sensitized Solar Cells, *Phys. Chem. Chem. Phys.*, 2012, **14**(22), 7934.

57 M. L. Mueller, X. Yan, B. Dragnea and L. Li, Slow Hot-Carrier Relaxation in Colloidal Graphene Quantum Dots, *Nano Lett.*, 2011, **11**(1), 56–60.

58 M. L. Mueller, X. Yan, J. A. McGuire and L.-S. Li, Triplet States and Electronic Relaxation in Photoexcited Graphene Quantum Dots, *Nano Lett.*, 2010, **10**(7), 2679–2682.

59 H. Riesen, C. Wiebeler and S. Schumacher, Optical Spectroscopy of Graphene Quantum Dots: The Case of C132, *J. Phys. Chem. A*, 2014, **118**(28), 5189–5195.

60 K. J. Williams, C. A. Nelson, X. Yan, L.-S. Li and X. Zhu, Hot Electron Injection from Graphene Quantum Dots to TiO_2, *ACS Nano*, 2013, **7**(2), 1388–1394.